COMPARISON OF DIFFERENT PAN-SHARPENING METHODS APPLIED TO IKONOS IMAGERY

Emanuele ALCARAS[1]*, *Vincenzo DELLA CORTE*[2], *Giampaolo FERRAIOLI*[3], *Elena MARTELLATO*[3], *Pasquale PALUMBO*[3], *Claudio PARENTE*[3], *Alessandra ROTUNDI*[3]

DOI : 10.21163/GT_2021.163.15

ABSTRACT :
On board the IKONOS satellite there are sensors operating in the panchromatic and multispectral range: the geometric resolution of the acquired images is higher in the first case (1 m) than in the second one (4 m); on the contrary, panchromatic images have lower spectral resolution than the latter. Pan-sharpening methods allow to reduce the pixel dimensions of the multispectral images to comply with the panchromatic resolution. In this way, it is possible to obtain enhanced detailed data in both geometric and spectral resolution. This work aims to compare the results obtained from the application of eight different pan-sharpening methods, which are totally carried out by using the raster calculator in QGIS: Multiplicative, Simple Mean, Brovey Transformation, Brovey Transformation Fast, Intensity Hue Saturation (IHS), IHS Fast, Gram-Schmidt, and Gram-Schmidt Fast. Each resulting dataset is compared with the original one to evaluate the performance of each method by the following quality indices: Correlation Coefficient (CC), Universal Image Quality Index (UIQI), Relative Average Spectral Error (RASE), Erreur Relative Global Adimensionnelle de Synthèse (ERGAS), Spatial Correlation Coefficient (SCC) and Spatial ERGAS (SERGAS); however, this is a difficult task because the quality of the fused image depends on the considered datasets. Finally, a comparison the various between methods is carried out.

Key-words: *Data fusion, Pan-sharpening, IKONOS, GIS-Application, VHR.*

1. INTRODUCTION

In the last twenty years satellite images with high geometric resolution have found great diffusion in remote sensing applications, such as in data fusion applications (Zhang, 2010). Particularly, data fusion is defined as the combination of data of different kind or source in order to obtain new information (Boulkaboul & Djenouri, 2020), which is referred to as “image fusion” when derived from images. Image fusion is defined as the combination of two or more images, through the use of algorithms, to form a new one synthetizing the characteristics of the inputs (Belgiu & Stein, 2019). If the aim of the image fusion is to inoculate geometric resolution of the panchromatic data (PAN) in each multispectral image (MS_i) preserving its spectral resolution, then it is referred as pan-sharpening (Tomas et al., 2008; Pal et al., 2019).

Usually, image fusion techniques can be classified in three levels: pixel level, feature level and decision level (Abdikan et al., 2014). Among them the most interesting for remote sensing are the pixel level techniques, since they permit the lowest alteration of the input dataset and thus most pan-sharpening methods fall back in this category (Wald & Ranchin, 1997; Zhang, 2004).

**Corresponding Author*
[1]*International PhD Programme “Environment, Resources and Sustainable Development”, Department of Science and Technology, Parthenope University of Naples, Centro Direzionale, Isola C4, (80143) Naples, Italy, emanuele.alcaras@uniparthenope.it*
[2]*IAPS—INAF, Via del Fosso del Cavaliere 100, 00133 Rome, Italy, vincenzo.dellacorte@inaf.it*
[3]*DIST - Department of Science and Technology, Parthenope University of Naples, Centro Direzionale, Isola C4, (80143) Naples, Italy, giampaolo.ferraioli@uniparthenope.it, elena.martellato@collaboratore.uniparthenope.it, pasquale.palumbo@uniparthenope.it, claudio.parente@uniparthenope.it, rotundi@uniparthenope.it*

Pixel level techniques can be either divided in three further categories: colour-related methods, statistics methods and numerical methods (Pohl & van Genderen, 1998). Intensity Hue Saturation (IHS) and IHS Fast (IHSF) methods belong to the first class, Gram-Schmidt (GS) and Gram-Schmidt Fast (GSF) belong to the second class, and Simple-Mean (SM), Multiplicative (MLT), Brovey Transformation (BT), Brovey Transofrmation Fast (BTF), which include arithmetic operations such as sum or multiplication between images, belong to the third class (Ehlers et al., 2010).

The results need to be analysed and compared to evaluate the performance of each technique; in order to achieve this scope several studies have been conducted so far (Du et al., 2007; Yuhendra & Kuze, 2011; Choi et al., 2019). Since no reference multispectral image with the same resolution of the fused image exist, it is difficult to define the accuracy of the pan-sharpening application (Parente & Pepe, 2017). Therefore, several methods and indices have been suggested and still under evaluation for the technique performance review (Meng et al., 2019). Among the most diffused indices for assessing pan-sharpening efficiency some can be categorized as spectral index, such as the Correlation Coefficient (CC), Universal Image Quality Index (UIQI), Relative Average Spectral Error (RASE), Erreur Relative Globale Adimensionalle de Synthèse (ERGAS), and some as spatial index, such as the Spatial Correlation Coefficient (SCC) and the spatial ERGAS (SERGAS). The first group remarks the spectral difference introduced by the pan-sharpening between the fused image and the initial MS image (Shahdoosti & Ghassemian, 2014). The second group remarks the conservation level of the spatial details assured by the pan-sharpening in terms of similarity between the object contours in the fused image and the corresponding one in the panchromatic image (Alcaras et al, 2021). Pan-sharpening techniques can be applied in many fields such as cultural heritage preservation (Baiocchi et al., 2017), shadow detection (Meneghini & Parente, 2015), vegetation mapping (Ibarrola-Ulzurrun et al., 2017), urban development (Hu et al., 2015), coastline evolution (Maglione et al., 2015), etc.

In this study, IKONOS imagery are considered and briefly introduced in the first section; next, eight methods, used to apply pan-sharpening to the original dataset, are explained; consequentially, evaluation indices are applied to the pan-sharpened images and discussed; finally, conclusions are provided in order to remark the importance of the work. All the operations have been carried out in QGIS.

2. DATASET

In this work image fusion techniques are performed on IKONOS imagery.

IKONOS was a commercial high-resolution imaging satellite of DigitalGlobe, launched on September 24, 1999, and retired in 2015. It was equipped with two sensors, which acquired images in panchromatic band with a resolution of 0.8 m (nadir), with a nominal Ground Sampling Distance (GSD)of 1 m, and in multispectral bands with a radiometric resolution of 11 bit and a spatial resolution of 3.2 m (nadir), nominal GSD of 4 m (Amato et al., 2004; DigitalGlobe, 2019).

Table 1 synthetizes the characteristics of IKONOS images (ESA, IKONOS Product Guide, 2006).

Table 1.

Band range of IKONOS satellite imagery.

IKONOS		
Bands	**Wavelength Range (μm)**	**Geometric Resolution (m)**
Panchromatic	0.526 - 0.929	1
Band 1 - Blue	0.445 - 0.516	4
Band 2 - Green	0.506 - 0.595	4
Band 3 - Red	0.632 - 0.698	4
Band 4 - Near Infrared	0.757 - 0.853	4

For this study, an IKONONS scene acquired on 18/01/2005 at 04:23 GMT is selected. The scene concerns a coastal area in the north of Indonesia as shown in **Fig. 1**.

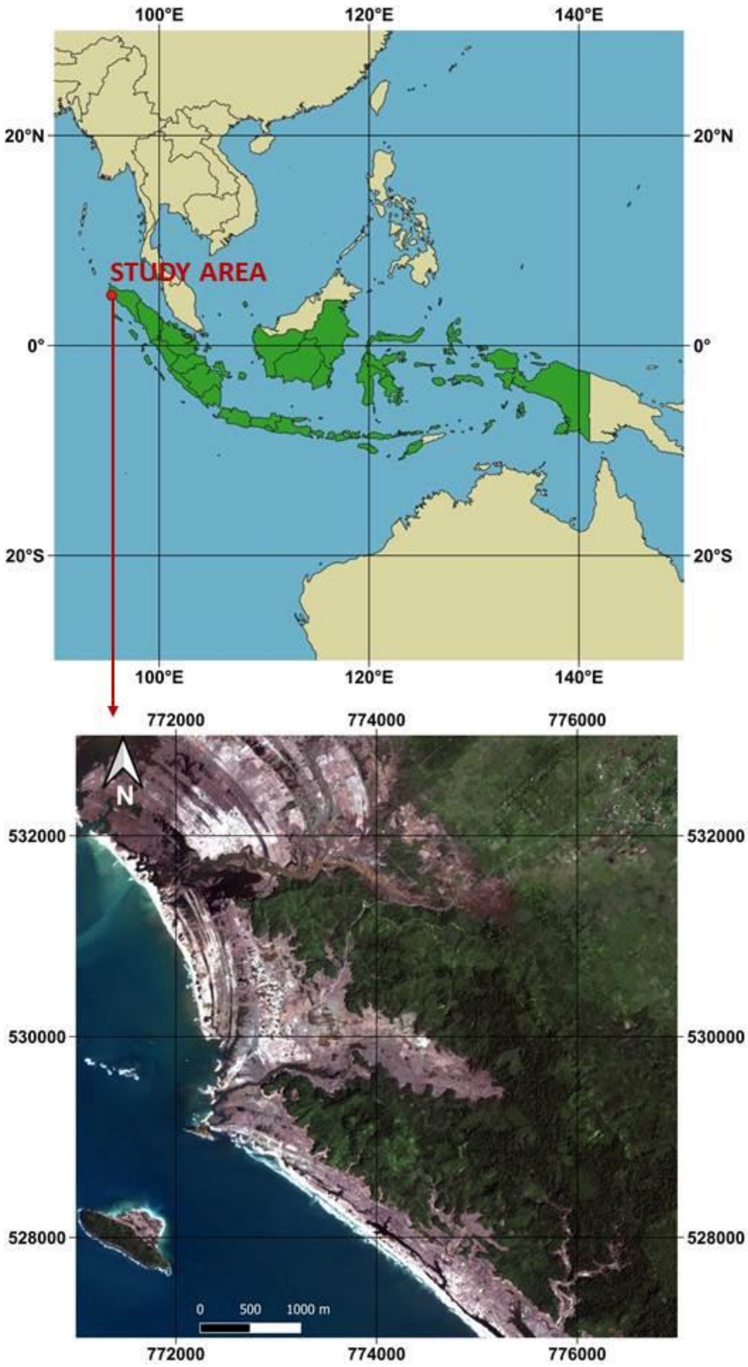

Fig. 1. The location of the study area relatively to Indonesia (*upper*) and RGB true colour composition, obtained with bands 3,2,1, of the considered IKONOS scene (*lower*).

The study area has an extension of 36 km^2 (6 km x 6 km). Particularly, this area extends within the following UTM/WGS84 plane coordinates – 46 zone in the north hemisphere: E_1 = 771,000 m, E_2 = 777,000 m, N_1 = 527,000 m, N_2 = 533,000 m.

3. METHODOLOGY

For our performance analysis eight pan-sharpening methods are applied to the IKONOS dataset to achieve the image fusion. The outputs of pan-sharpening application are therefore evaluated by means of spectral indicators (CC, UIQI, RASE, ERGAS) and spatial indicators (SCC, SERGAS). The operations are totally carried out by using the raster calculator tool in QGIS, version 3.16.1 (QGIS, Working with Raster Data, 2020).

3.1. Pan-sharpening Methods

The pan-sharpening methods here considered have been widely used in the image-fusion field and they are described in the following subsections.

3.1.1. Multiplicative (MLT)

The i-th pan-sharpened image (MS_i') is obtained from the following formula:

$$MS_i' = \frac{PAN}{\mu_{PAN}} MS_i \tag{1}$$

where μ_{PAN} is the mean reflectance value of the panchromatic image (PAN) (Crippen, 1987).

3.1.2. Simple Mean (SM)

This method applies a simple arithmetic mean between the i-th multispectral image and the panchromatic image (ESRI, Fundamentals of panchromatic sharpening, 2020). The i-th pan-sharpened image is given by:

$$MS_i' = \frac{PAN + MS_i}{2} \tag{2}$$

3.1.3. Intensity Hue Saturation (IHS)

This pan-sharpening method is based on a RGB colour model to Intensity – Hue – Saturation (IHS) model transformation. The IHS method was introduced by Carper et al. (Carper et al., 1990), and furtherly extended by Tu et al. (Tu et al., 2001) by including the near-infrared (NIR) band into the intensity component. In particular, given *N* multispectral bands, Intensity (I) can be computed as a synthetic band, given by the following formula:

$$I = \frac{\sum_{i=1}^{N} MS_i}{N} \tag{3}$$

3.1.4. IHS Fast (IHSF)

A variation of IHS method can be achieved if specific weights are introduced for each MS_i (Tu et al., 2004):

$$I = \frac{\sum_{i=1}^{N} w_i MS_i}{\sum_{i=1}^{N} w_i} \tag{4}$$

where w_i are the weights.

For IKONOS images the weights are typically 0.08 for Blue, 0.25 for Green, 0.33 for Red and 0.33 for NIR (Aiazzi et al., 2007), and they can be also estimated from the spectral response in **Fig. 2**.

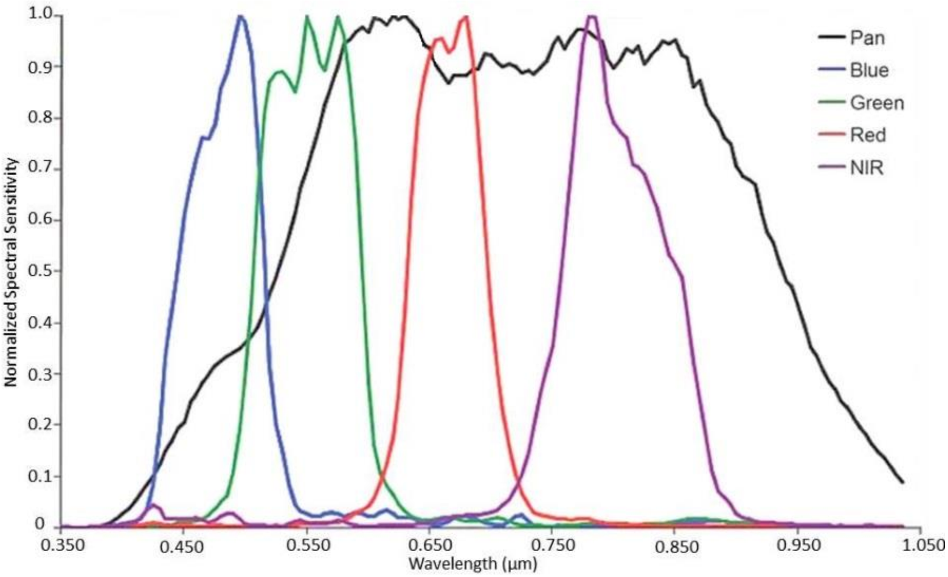

Fig. 2. Spectral response of the IKONOS MS and PAN sensors.

3.1.5. Brovey Transformation (BT)

The Brovey pan-sharpened image can be computed as described by Pohl and van Genderen (Pohl & van Genderen 1998):

$$MS_i' = \frac{PAN}{\frac{1}{N}\sum_{i=1}^{N} MS_i} MS_i \tag{5}$$

3.1.6. Brovey Transformation Fast (BTF)

As for the IHSF method, the same weights can be introduced in for BT:

$$MS_i^i = \frac{PAN}{\sum_{i=1}^{N} w_i\, MS_i} MS_i \sum_{i=1}^{N} w_i \tag{6}$$

3.1.7. Gram-Schmidt (GS)

In the Gram-Schmidt method the pan-sharpened image can be achieved through the subsequent steps:

- Creation of a lower resolution panchromatic image, which is called Simulated panchromatic (S) as the linear combination of the N MS_i bands;
- Application of the Gram-Schmidt orthogonalization starting from S, which is employed as the first band of the transformation;
- Once all the bands are de-correlated, S can be substituted by the high-resolution panchromatic image and the inverse Gram-Schmidt transformation is applied to obtain the pan-sharpened images (Laben & Brower, 2000).

Ultimately, the pan-sharpened image is given by:

$$MS_i' = MS_i + g_i(PAN - S) \tag{7}$$

where, g_i is called gain and is given by:

$$g_i = \frac{cov(MS_i, S)}{var(S)} \tag{8}$$

where $cov(MS_i, S)$ is the covariance between the initial i-th multispectral image and the low resolution panchromatic image; $var(S)$ is S variance.

3.1.8. Gram-Schmidt Fast (GSF)

As in formulas (4) and (6), weights can also be introduced in this method (Maurer, 2013), and S will be obtained as follow:

$$S = \sum_{i=1}^{N} w_i MS_i \tag{9}$$

3.2. Pan-sharpening evaluation

The performance of each method is now evaluated by comparing the original image with the corresponding pan-sharpened image. However, this evaluation is a difficult task: even if the performance of some methods is limited, the quality of the pan-sharpening method cannot be established in an absolute way because it also depends on the considered datasets (Snehmani et al., 2017). As a consequence, different methods are initially applied, and the final image is then the most performant among the resulting pan-sharpened images.

The evaluation task can be carried out in terms of visual, spectral and spatial quality analysis. A visual inspection of the resulting images allows to assess the capability of the method to preserve the colour and to improve the spatial resolution of the represented object (Wang & Bovik, 2002). Spectral analysis, based on appositive indices, is required to establish the spectral similarity between MS and the corresponding MS'. Spatial analysis, also based on appositive indices, is useful to derive the similarities between the shape of the objects included in the MS' and the corresponding one in the PAN (Alcaras et al., 2021).

A brief description of each quality index and spatial index used in this application is reported below.

- *Correlation Coefficient (CC)*

Correlation between two bands is measured, particularly the original image (x) and corresponding pan-sharpened image (y) are compared. CC is given by the following formula (Meng et al., 2016):

$$CC = \frac{\sigma_{xy}}{\sigma_x \sigma_y} \tag{10}$$

where, σ_{xy} is the covariance between x and y images, σ_x and σ_y are the standard deviation of x and y images, respectovely. The closer to 1 is CC the more correlated are x and y (Vijayaraj et al., 2004).

- *Universal Image Quality Index (UIQI)*

It is a product of three components, given by the following formula:

$$UIQI = \frac{\sigma_{xy}}{\sigma_x \sigma_y} \cdot \frac{2\mu_x \mu_y}{\mu_x^2 + \mu_y^2} \cdot \frac{2\sigma_x \sigma_y}{\sigma_x^2 + \sigma_y^2} \tag{11}$$

where μ_x and μ_y are the mean values of x and y images, respectively (Wang & Bovik, 2002). The first component is CC; the second component takes into account the shift of the mean values between x and y; the third component evaluates the similarity of the contrast between the x and y. The closer to 1 is UIQI the more correlated are x and y (Nikolakopoulos & Oikonomidis, 2015).

- *Relative Average Spectral Error (RASE)*

This index includes all the N bands in the formula:

$$RASE = \frac{100}{M}\sqrt{\frac{1}{N}\sum_{i=1}^{N}(RMSE_i)^2} \quad (12)$$

where, M is the mean value of Digital Numbers of the N input images; $RMSE_i$ is the root mean square error between the original i-th image and the corresponding i-th fused image (Ranchin & Wald, 2000). The littler the index the better the quality of the image fusion is.

- *Erreur Relative Globale Adimensionalle de Synthèse (ERGAS)*

It quantifies the spectral quality of the fused images with the following formula:

$$ERGAS = 100\frac{h}{l}\sqrt{\frac{1}{N}\sum_{i=1}^{N}\left(\frac{RMSE_i}{\mu_i}\right)^2} \quad (13)$$

where, h is PAN spatial resolution; l is MS_i spatial resolution; μ_i is the mean radiance value of the i-th band (Wald, 2000). The littler the index the better the quality of the image fusion.

- *Spatial Correlation Coefficient (SCC)*

Similarly, to CC, SCC measures the correlation between two bands, which are the panchromatic (p) and the fused images (y), obtaining better results when the values are close to one (Li et al., 2002):

$$SCC = \frac{\sigma_{py}}{\sigma_p \sigma_y} \quad (14)$$

where, σ_{py} is the covariance between p and y images, σ_p and σ_y are the standard deviation of p and y images, respectively.

- *Spatial ERGAS (SERGAS)*

To quantify the spatial quality of the fused images, ERGAS can be modified by substituting the RMSE with the spatial RMSE (SRMSE):

$$SERGAS = 100\frac{h}{l}\sqrt{\frac{1}{N}\sum_{i=1}^{N}\left(\frac{SRMSE_i}{\mu_i}\right)^2} \quad (15)$$

where $SRMSE_i$ is the root mean square error between PAN image and the corresponding i-th fused image (Lillo-Saavedra et al., 2005).

4. RESULTS AND DISCUSSIONS

To show the results of image fusion operations computed by QGIS Raster Calculator, a detail of the study area is selected (**Fig. 3**). The fused images and original bands are compared and shown in the detailed scene RGB compositions in **Fig. 4**.

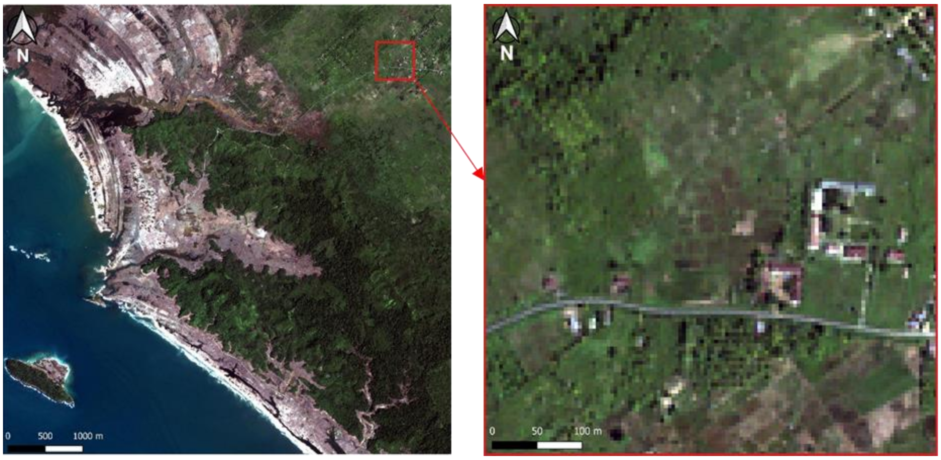

Fig. 3. The red square, in the left image, represents the chosen detail area, reported in the right image.

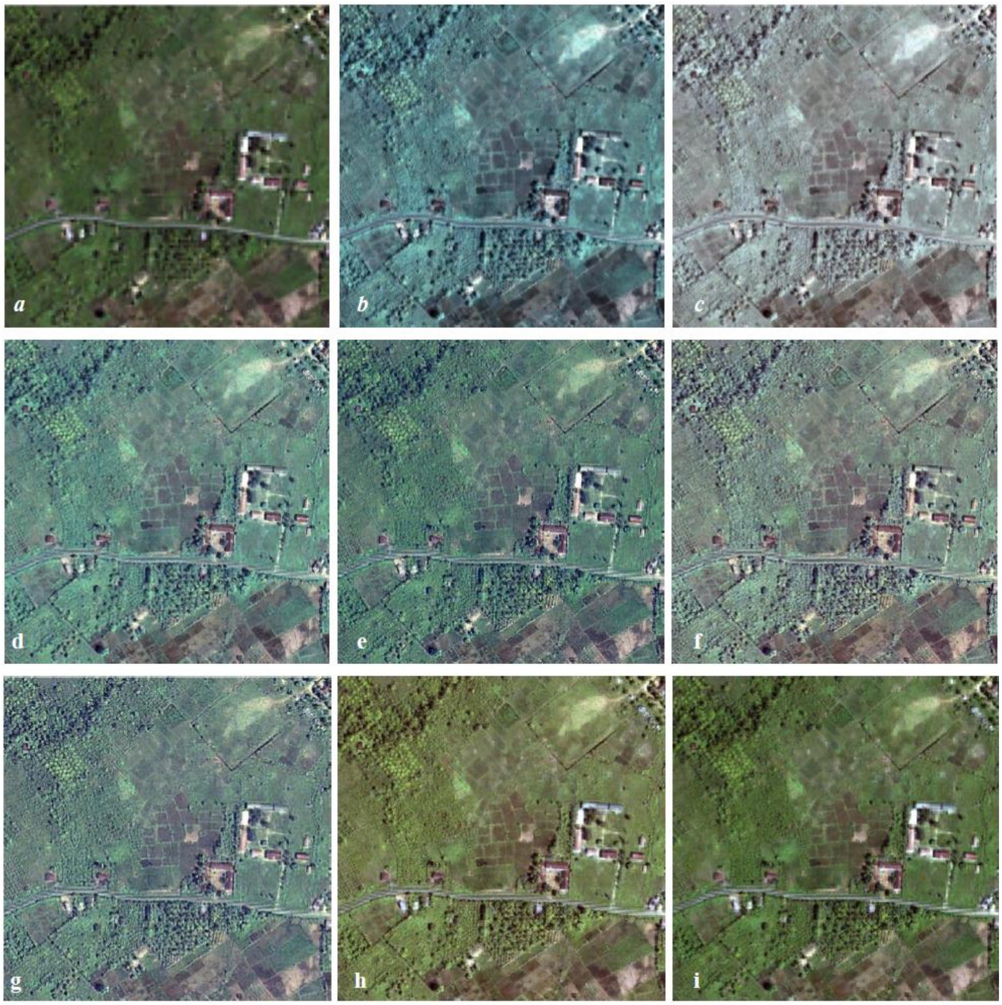

Fig. 4. RGB composition of the original images (a) and RGB compositions of the images derived by the following methods: (b) MLT, (c) SM, (d) BT, (e) BTF, (f) IHS, (g) IHSF, (h) GS and (i) GSF.

In most cases, the colours given by the RGB compositions look natural or simile natural, except for Multiplicative and Simple Mean methods.

The results of the quality evaluation process of the pan-sharpening techniques are reported below, including the values of the adopted indices in the following order: CC (**Tab 2**), UIQI (**Tab. 3**), RASE (**Tab. 4**), ERGAS (**Tab. 5**), SCC (**Tab. 6**) and SERGAS (**Tab. 7**). Particularly, for CC, UIQI and SCC, mean values for each method are provided in the last row.

Table 2.

CC values for pan-sharpened images.

CC								
Bands	**MLT**	**SM**	**BT**	**BTF**	**IHS**	**IHSF**	**GS**	**GSF**
Blue	0.649	0.517	0.512	0.657	0.487	0.597	0.945	0.980
Green	0.829	0.756	0.759	0.824	0.751	0.796	0.768	0.958
Red	0.897	0.829	0.930	0.945	0.844	0.873	0.894	0.955
NIR	0.949	0.989	0.964	0.962	0.990	0.988	0.951	0.944
Mean	0.831	0.773	0.791	0.847	0.768	0.813	0.889	**0.959**

Table 3.

UIQI values for pan-sharpened images.

UIQI								
Bands	**MLT**	**SM**	**BT**	**BTF**	**IHS**	**IHSF**	**GS**	**GSF**
Blue	0.345	0.483	0.484	0.648	0.466	0.583	0.944	0.980
Green	0.517	0.751	0.743	0.821	0.740	0.794	0.753	0.958
Red	0.708	0.809	0.928	0.942	0.835	0.870	0.890	0.954
NIR	0.819	0.920	0.949	0.960	0.981	0.986	0.902	0.934
Mean	0.597	0.741	0.776	0.843	0.755	0.808	0.872	**0.956**

Table 4.

RASE values for pan-sharpened images.

RASE							
MLT	**SM**	**BT**	**BTF**	**IHS**	**IHSF**	**GS**	**GSF**
52.781	27.737	24.825	20.531	21.939	**18.880**	28.450	20.756

Table 5.

ERGAS values for pan-sharpened images.

ERGAS							
MLT	**SM**	**BT**	**BTF**	**IHS**	**IHSF**	**GS**	**GSF**
14.644	7.144	5.633	4.571	5.968	5.072	5.787	**4.005**

Table 6.
SCC values for pan-sharpened images.

SCC								
Bands	**MLT**	**SM**	**BT**	**BTF**	**IHS**	**IHSF**	**GS**	**GSF**
Blue	0.842	0.943	0.867	0.634	0.814	0.530	0.447	0.282
Green	0.804	0.919	0.873	0.730	0.852	0.681	0.635	0.571
Red	0.697	0.900	0.734	0.658	0.832	0.705	0.789	0.640
NIR	0.922	0.932	0.901	0.912	0.895	0.897	0.908	0.908
Mean	0.816	**0.924**	0.844	0.733	0.848	0.703	0.695	0.600

Table 7.
SERGAS values for pan-sharpened images.

SERGAS							
MLT	**SM**	**BT**	**BTF**	**IHS**	**IHSF**	**GS**	**GSF**
18.286	**7.144**	12.966	13.220	12.186	13.232	13.878	13.844

Tables from 2 to 5 report values of indices assessing the spectral quality of the pan-sharpened images.

Considering results by CC (**Tab. 2**), GSF is the most performing method, while IHS presents the lowest value. Considering results by UIQI (**Tab. 3**), GSF is still the most performing method, MLT is the worst performing. Considering results by RASE (**Tab. 4**), this is the only case in which GSF is not the most performing method since it is overridden by IHSF (most performing) and BTF; MLT is still the worst performing method. Considering results by ERGAS (**Tab. 5**), GSF is again the most performing method, while MLT is once more the worst performing one.

By considering the only spectral indicators, we can observe that GSF is the best method among the eight considered ones, BTF also gives a good response (it always falls in the top three methods), while MLT and SM are the worst methods in most cases.

It is also clear that the “fast” methods, so the ones using the weights, are better performant than the respective not weighted ones, in accordance with what found also by other authors (Fasbender et al., 2008; Amro et al., 2011; Maglione et al., 2016).

Tables 6 and 7 report values of indices assessing the spatial quality of the pan-sharpened images.

Considering results by SCC (**Tab. 6**), SM shows higher values, being the only method with a mean value of SCC above 0.900, while GS and GSF performances are quite low. Considering results by SERGAS (**Tab. 7**), SM is once again the most performing method by far while MLT provides inaccurate results. From the comparison of the values obtained in **Tables 6 and 7**, we found that SM is the most performing method if the only spatial quality is considered, followed by IHS and BT. The “fast” methods performances are always lower than the corresponding non-weighted methods.

The experiment results confirm that the choice of the best method is a challenging and non-univoque task, and it depends on the needs of the user. For consequence, as reported in Alcaras et al., (2021), a multi-criteria analysis can be carried out to choose the most suitable method depending on the situation.

5. CONCLUSIONS

Starting from an IKONOS imagery dataset, in this paper eight different pan-sharpening methods are evaluated. Since the IKONOS imagery dataset provides five images (four multispectral images and one panchromatic image), by applying eight pan-sharpening methods, a total of thirty-two new images are obtained. The investigated algorithms are: SM, MLT, IHS, IHSF, BT, BTF, GS and GSF.

Once the outputs are available, each method is tested by comparing the fused images with the initial dataset. In order to evaluate each method 6 different indices are used: CC, UIQI, RASE, ERGAS, SCC and SERGAS. In this way a comparison between different algorithms is possible.

Two methods, which are SM and especially MLT, produce high radiometric distortions on the output. For the other six methods a distinction could be made between the no-weighted and weighted methods: the latter always provide better results in terms of spectral fidelity, and among the three weighted methods, GSF results the most performing one, followed by BTF.

On the other hand, by assessing spatial quality of the fusion products, the performances of the methods behave reversely: SM is the best method and the fast methods do not provide good results.

Evaluating the quality of pan-sharpening products can be a challenging matter, so it is important to use all visual, spectral and spatial quality analyses, to find the better product that meets the user needs.

REFERENCES

Abdikan, S., Balik Sanli, F., Sunar, F., & Ehlers, M. (2014). A comparative data-fusion analysis of multi-sensor satellite images. *International Journal of Digital Earth*, *7*(8), 671-687. https://doi.org/10.1080/17538947.2012.748846

Aiazzi, B., Baronti, S., & Selva, M. (2007). Improving component substitution pansharpening through multivariate regression of MS $+ $ Pan data. *IEEE Transactions on Geoscience and Remote Sensing*, *45*(10), 3230-3239. https://doi.org/10.1109/TGRS.2007.901007

Alcaras, E., Parente, C., & Vallario, A. (2021). Automation of Pan-Sharpening Methods for Pléiades Images Using GIS Basic Functions. *Remote Sensing*, 13(8), 1550. https://doi.org/10.3390/rs13081550

Amato, R., Dardanelli, G., Emmolo, D., Franco, V., Brutto, M. L., Midulla, P., ... & Villa, B. (2004). Digital orthophotos at a scale of 1: 5000 from high resolution satellite images. *ISPRS Journal of Photogrammetry & Remote Sensing*, 35, 593-598.

Amro, I., Mateos, J., Vega, M., Molina, R., & Katsaggelos, A. K. (2011). A survey of classical methods and new trends in pansharpening of multispectral images. *EURASIP Journal on Advances in Signal Processing*, *2011*(1), 1-22. https://doi.org/10.1186/1687-6180-2011-79

Baiocchi, V., Bianchi, A., Maddaluno, C., & Vidale, M. (2017). Pansharpening techniques to detect mass monument damaging in Iraq. *International Archives of the Photogrammetry, Remote Sensing & Spatial Information Sciences*, 42.

Belgiu, M., & Stein, A. (2019). Spatiotemporal image fusion in remote sensing. *Remote sensing*, *11*(7), 818. https://doi.org/10.3390/rs11070818

Boulkaboul, S., & Djenouri, D. (2020). DFIOT: data fusion for Internet of Things. *Journal of Network and Systems Management*, 1-25. https://doi.org/10.1007/s10922-020-09519-y

Carper, W., Lillesand, T., & Kiefer, R. (1990). The use of intensity-hue-saturation transformations for merging SPOT panchromatic and multispectral image data. *Photogrammetric Engineering and remote sensing*, *56*(4), 459-467.

Choi, J., Park, H., Seo, D., & Han, Y. (2019). Performance Analysis of Pansharpening Algorithms Based on Guided Filtering Applied to KOMPSAT-3/3A Satellite Imagery in Coastal Areas. *Journal of Coastal Research*, *91*(SI), 431-435. https://doi.org/10.2112/SI91-087.1

Crippen, R. E. (1989). A simple spatial filtering routine for the cosmetic removal of scan-line noise from Landsat TM P-tape imagery. *Photogrammetric Engineering and Remote Sensing*, *55*(3), 327-331.

DigitalGlobe, 2019. IKONOS Data Sheet https://dg-cms-uploads-production.s3.amazonaws.com/uploads/document/file/96/DG_IKONOS_DS.pdf (Accessed on: May 02, 2020)

Du, Q., Younan, N. H., King, R., & Shah, V. P. (2007). On the performance evaluation of pan-sharpening techniques. *IEEE Geoscience and Remote Sensing Letters*, *4*(4), 518-522. https://doi.org/10.1109/LGRS.2007.896328

Ehlers, M., Klonus, S., Johan Åstrand, P., & Rosso, P. (2010). Multi-sensor image fusion for pansharpening in remote sensing. *International Journal of Image and Data Fusion*, *1*(1), 25-45. https://doi.org/10.1080/19479830903561985

ESA, IKONOS Product Guide, 2006 https://earth.esa.int/eogateway/documents/20142/37627/IKONOS-Imagery-Product-Guide.pdf (Accessed on: March 18, 2021)

ESRI, Fundamentals of panchromatic sharpening, ArcGIS 10.3-Help, Redlands, CA, USA, 2020. https://desktop.arcgis.com/en/arcmap/10.3/manage-data/raster-and-images/fundamentals-of-panchromatic-sharpening.htm (Accessed on: May 05, 2020)

Fasbender, D., Radoux, J., & Bogaert, P. (2008). Bayesian data fusion for adaptable image pansharpening. *IEEE Transactions on Geoscience and Remote Sensing*, *46*(6), 1847-1857. https://doi.org/10.1109/TGRS.2008.917131

Hu, Y., Jia, G., Pohl, C., Feng, Q., He, Y., Gao, H., ... & Feng, J. (2015). Improved monitoring of urbanization processes in China for regional climate impact assessment. *Environmental Earth Sciences*, *73*(12), 8387-8404. https://doi.org/10.1007/s12665-014-4000-4

Ibarrola-Ulzurrun, E., Gonzalo-Martín, C., & Marcello, J. (2017). Influence of pansharpening in obtaining accurate vegetation maps. Canadian Journal of Remote Sensing, 43(6), 528-544. https://doi.org/10.1080/07038992.2017.1371583

Laben, C. A., & Brower, B. V. (2000). *U.S. Patent No. 6,011,875*. Washington, DC: U.S. Patent and Trademark Office.

Li, S., Kwok, J.T., & Wang, Y. (2002). Using the discrete wavelet frame transform to merge Landsat TM and SPOT panchromatic images. Inf. Fusion, (3), 17‑23.

Lillo-Saavedra, M., Gonzalo, C., Arquero, A., & Martinez, E. (2005). Fusion of multispectral and panchromatic satellite sensor imagery based on tailored filtering in the Fourier domain. International Journal of Remote Sensing, 26(6), 1263-1268. https://doi.org/10.1080/01431160412331330239

Maglione, P., Parente, C., & Vallario, A. (2015). High resolution satellite images to reconstruct recent evolution of domitian coastline. American Journal of Applied Sciences, 12(7), 506. https://doi.org/10.3844/ajassp.2015.506.515

Maglione, P., Parente, C., & Vallario, A. (2016). Pan-sharpening WorldView-2: IHS. *Brovey and Zhang methods in comparison*, *8*(2), 673-679.

Maurer, T. (2013). How to pan-sharpen images using the gram-schmidt pan-sharpen method–A recipe. *International archives of the photogrammetry, remote sensing and spatial information sciences*, *1*, W1. https://doi.org/10.5194/isprsarchives-XL-1-W1-239-2013

Meneghini, C., & Parente, C. (2015). Application for shadow removal from GeoEye-1 RGB composition. *International Journal of Applied Engineering Research*, *10*(6), 15833-15842.

Meng, X., Li, J., Shen, H., Zhang, L., & Zhang, H. (2016). Pansharpening with a guided filter based on three-layer decomposition. *Sensors*, *16*(7), 1068. https://doi.org/10.3390/s16071068

Meng, X., Shen, H., Li, H., Zhang, L., & Fu, R. (2019). Review of the pansharpening methods for remote sensing images based on the idea of meta-analysis: Practical discussion and challenges. *Information Fusion*, *46*, 102-113. https://doi.org/10.1016/j.inffus.2018.05.006

Nikolakopoulos, K., & Oikonomidis, D. (2015). Quality assessment of ten fusion techniques applied on Worldview-2. *European Journal of Remote Sensing*, *48*(1), 141-167. https://doi.org/10.5721/EuJRS20154809

Pal, M. K., Rasmussen, T. M., & Abdolmaleki, M. (2019, September). Multiple Multi-Spectral Remote Sensing Data Fusion and Integration for Geological Mapping. In *2019 10th Workshop on Hyperspectral Imaging and Signal Processing: Evolution in Remote Sensing (WHISPERS)* (pp. 1-5). IEEE. https://doi.org/10.1109/WHISPERS.2019.8921142

Parente, C., & Pepe, M. (2017). Influence of the weights in IHS and Brovey methods for pan-sharpening WorldView-3 satellite images. *International Journal of Engineering & Technology*, *6*(3), 71-77. https://doi.org/10.14419/ijet.v6i3.7702

Pohl, C., & Van Genderen, J. L. (1998). Review article multisensor image fusion in remote sensing: concepts, methods and applications. *International journal of remote sensing*, *19*(5), 823-854. https://doi.org/10.1080/014311698215748

QGIS 2.8 Documentation, QGSI User Guide, Working with Raster Data, 2020. https://docs.qgis.org/2.8/en/docs/user_manual/working_with_raster/raster_calculator.html (Accessed on: May 05, 2020)

Ranchin, T., & Wald, L. (2000). Fusion of high spatial and spectral resolution images: The ARSIS concept and its implementation. *Photogrammetric engineering and remote sensing*, *66*(1), 49-61.

Shahdoosti, H. R., & Ghassemian, H. (2014). Fusion of MS and PAN images preserving spectral quality. *IEEE Geoscience and Remote Sensing Letters*, 12(3), 611-615. https://doi.org/10.1109/LGRS.2014.2353135

Snehmani, Gore, A., Ganju, A., Kumar, S., Srivastava, P. K., & RP, H. R. (2017). A comparative analysis of pansharpening techniques on QuickBird and WorldView-3 images. *Geocarto International*, *32*(11), 1268-1284. https://doi.org/10.1080/10106049.2016.1206627

Thomas, C., Ranchin, T., Wald, L., & Chanussot, J. (2008). Synthesis of multispectral images to high spatial resolution: A critical review of fusion methods based on remote sensing physics. *IEEE Transactions on Geoscience and Remote Sensing*, *46*(5), 1301-1312. https://doi.org/10.1109/TGRS.2007.912448

Tu, T. M., Huang, P. S., Hung, C. L., & Chang, C. P. (2004). A fast intensity-hue-saturation fusion technique with spectral adjustment for IKONOS imagery. *IEEE Geoscience and Remote sensing letters*, *1*(4), 309-312. https://doi.org/10.1109/LGRS.2004.834804

Tu, T. M., Su, S. C., Shyu, H. C., & Huang, P. S. (2001). A new look at IHS-like image fusion methods. *Information fusion*, *2*(3), 177-186. https://doi.org/10.1016/S1566-2535(01)00036-7

Vijayaraj, V., O'Hara, C. G., & Younan, N. H. (2004, September). Quality analysis of pansharpened images. In *IGARSS 2004. 2004 IEEE International Geoscience and Remote Sensing Symposium* (Vol. 1). IEEE. https://doi.org/10.1109/IGARSS.2004.1368951

Yuhendra, J., Kuze, H., & Sri Sumantyo, J. (2011). Performance analyzing of high resolution pan-sharpening techniques: increasing image quality for classification using supervised kernel support vector machine. *Research Journal of Information Technology*, *3*(1), 12-23. https://doi.org/10.3923/rjit.2011.12.23

Wald, L. (2000, January). Quality of high resolution synthesised images: Is there a simple criterion?. In *Third conference" Fusion of Earth data: merging point measurements, raster maps and remotely sensed images"* (pp. 99-103). SEE/URISCA.

Wald, L., Ranchin, T., & Mangolini, M. (1997). Fusion of satellite images of different spatial resolutions: Assessing the quality of resulting images. *Photogrammetric engineering and remote sensing*, *63*(6), 691-699.

Wang, Z., & Bovik, A. C. (2002). A universal image quality index. *IEEE signal processing letters*, *9*(3), 81-84. https://doi.org/10.1109/97.995823

Zhang, J. (2010). Multi-source remote sensing data fusion: status and trends. *International Journal of Image and Data Fusion*, *1*(1), 5-24. https://doi.org/10.1080/19479830903561035

Zhang, Y. (2004). System and method for image fusion. *United States Patent Application* No. 20040141659